



Grading evaluation of pore throats in a tight sandstone reservoir: a case study of the Gao 3 section reservoir in the Qijia area of the Songliao Basin

Qiang Yan^{1,2} · YiLin Li^{1,2} · YunFeng Zhang^{1,2}

Received: 15 November 2018 / Accepted: 30 August 2019 / Published online: 28 October 2019
© Saudi Society for Geosciences 2019

Abstract

The micropore throat of the Gao 3 section tight sandstone reservoir was studied using sampling and experimental (high-pressure mercury injection and scanning electron microscopy) methods. Based on the relative permeability, the reservoir can be divided into three categories: conventional, unconventional and low permeability. To determine the displacement pressure, porosity and other relevant parameters of various reservoirs, the mercury injection curve of all samples was projected to the same coordinate system. According to the position of the inflection point on the mercury injection curve of all levels of reservoirs, the pore throat was divided into three types: micropores, transition pores and macropores. Based on the theory that the throat is characterised by the mercury withdrawal curve, the throat in the present study is divided into three categories: the large throat, the medium throat and the small throat. Combined with the ordinate position at the inflection point, the critical point of micropore-throat classification of all kinds of reservoirs was determined. By analysing the histogram of pore-throat distribution of all kinds of reservoirs, the peak value of reservoir pore-throat distribution was determined. From the definition of expectation and variance in mathematics, the concept of grading parameters was introduced to determine the size and concentration degree of micropore-throat distribution at all levels of reservoirs, and a correlation analysis with permeability was performed to determine the control law of permeability.

Keywords High-pressure mercury injection · Tight sandstone · Grading evaluation · Grading parameters · Microscopic pore throat · Songliao Basin

Introduction

Tight oil, oil contained in geologic formations with low permeability, is currently an emerging hot spot in China's oil and gas exploration and development industry, much as shale gas

has been over the past decade. The successful commercial exploitation of tight oil in North America has demonstrated this resource's commercial value and changed the world energy pattern (Yan et al. 2017; Shejiao et al. 2014; Chengzao et al. 2012). Micropore throats have always been a difficult characteristic to define in reservoir research. Many domestic and international scholars have proposed methods and established models to characterise pore throat distribution (Dullien and Dhawan 1974; Hosseini et al. 2018; Wang et al. 2017). Accurate evaluation of the development of micropore throats in reservoirs is helpful for later resource evaluation and development (Rui et al. 2017). Zhu considers membership to be the linking factor of utilising the idea of information superposition, and combining the fuzzy comprehensive and grey relational evaluation methodologies into an uncertainty evaluation. The present study presents a differentiated and improved internal algorithm and establishes a more effective fuzzy-grey comprehensive evaluation method (Zhu et al. 2019). Zhenhua et al. (2018) created an index evaluation

Responsible Editor: Santanu Banerjee

✉ YiLin Li
liyilindaqing@163.com

Qiang Yan
412234179@qq.com

YunFeng Zhang
94073505@qq.com

¹ Department of Earth Sciences, Northeast Petroleum University, Daqing 163318, Heilongjiang, China

² Oil and Gas Reservoir Forming Mechanism and Resource Evaluation Key Laboratory, Daqing 163318, Heilongjiang, China

system to assess unconventional well readiness for development, which considers various well characteristics. Weyl and Beard (1973) investigated the relationship between porosity, permeability and texture of artificially mixed and packed sand to determine the approximate porosity and permeability values to be expected for unconsolidated sand of eight grain-size subclasses and six sorting groups.

China has recently discovered a large amount of tight oil and gas in the Ordos, Sichuan, Songliao, Junger and Bohai Bay basins, all of which have great exploration and development potential. At present, some exploration progress has been made, laying a foundation for large-scale effective development (Shejiao et al. 2014; Jianzhong et al. 2012). The term tight sandstone reservoir is used to describe any sandstone reservoir with porosity less than 12% and air permeability less than 1 mD (and in situ permeability less than 0.1 mD) (Chengzao et al. 2012). This is different from the evaluation criteria used for tight sandstone gas. The criterion for recognising tight gas sandstone reservoirs in China can be established as an in situ permeability of less than or equal to 0.1 mD with no natural commercial production (Caineng et al. 2015). The reservoir space is diversified; the micropore structure is complex; and the physical properties are poor, which makes exploration and development difficult. In particular, the complex microscopic pore structure (due to pore-throat size and distribution) has a decisive influence on the reservoir storage and seepage capacity, this has become a key and difficult point for further study of tight reservoirs (Yan et al. 2017). Junjian et al. (2018) have separated oil, water and particles accurately through image processing and established a pore network model to study the effect of heterogeneity of micropore-throat distribution on the residual oil distribution pattern.

At present, there are numerous technical methods that can characterise the micropore throats in a reservoir, but each method has some limitations. Therefore, it is necessary to integrate multiple technical methods to accurately and comprehensively characterise the pore throat distribution (Shuangfang et al. 2018; Caineng et al. 2015). Optical microscopy, scanning electron microscopy (SEM), cathodoluminescence and wireline log, core analysis permeability and porosity and production test data were applied to analyse the diagenesis and its controls on hydrocarbon potential in tight sandstone from the upper Triassic Chang 7 oil group of the Yanchang Formation, Ordos Basin, China (Yunlong et al. 2017). The standard classification of micropore throats includes Ходот and the International Union of Pure and Applied Chemistry (IUPAC) methods (IUPAC 1972; Ходот 1996). Ходот states that based on the principle of adsorption, the pore systems of coal can be divided into micropores (< 10 nm), small pores (10–100 nm), medium pores (100–1000 nm) and large pores (> 1000 nm). IUPAC classifies pores into three types: micropores (< 2 nm), medium

pores (2–50 nm) and large pores (> 50 nm). The former classification scheme is widely used in coal bed methane, whereas the latter is mainly used in shale gas (Shuangfang et al. 2018; Jian et al. 2015; Pengfei et al. 2017; Liu et al. 2018). However, the tight sandstone reservoirs have a broad variety of mineral compositions, grain sizes, structures, diageneses and development of microfractures. Therefore, based on existing classification schemes and the inflection point of the mercury injection curve, this paper will establish a microscopic pore-throat classification scheme that can accurately reflect its characteristics and internal laws, explain the grading evaluation criteria of tight reservoirs and attempt to apply the new classification scheme to evaluate tight reservoirs in the study area.

Geological setting

The Songliao Basin is one of the most oil-rich continental sedimentary basins in the world. Located on the Heilongjiang plate of the circum-Pacific tectonic domain (Fig. 1), this basin developed most of its sedimentary strata since the Mesozoic, and its Paleozoic strata is mostly basement rock. The study area is in the second and third sections of the upper Cretaceous Qingsankou formation, corresponding to the Gaotaizi formation. Four sets of oil-bearing layers developed from the Gaotaizi sub-reservoir formation. All the samples used in this experiment come from the third set of oil layers (Gao 3 section). The types of sedimentary facies found here include distributary channels, estuary bars, sheet sand and shallow lake bars (Yilin et al. 2016), and the sediments are mainly argillaceous siltstone and dark mudstone, with poor physical properties. The reservoir in the Gao 3 section is both source rock and reservoir, which is the composition of a typical tight reservoir.

Samples' characteristic and the method

Samples' characteristic

The samples for this experiment were sourced from the Gao 3 reservoir group. Results from core observations, scanning electron microscopy and casting thin section analysis show that in this area, the Gao 3 reservoir group is made up of lithic feldspar sandstone. According to thin section identification results, the main clastic components in the study area are quartz, feldspar and debris (Fig. 2), the proportions of quartz, feldspar and debris were relatively equal. Most of the pores were intergranular or dissolution pores, and organic pores did not develop.

As there are a large number of permeability data points that can be used for the high-pressure mercury injection experiment, several samples were selected in each

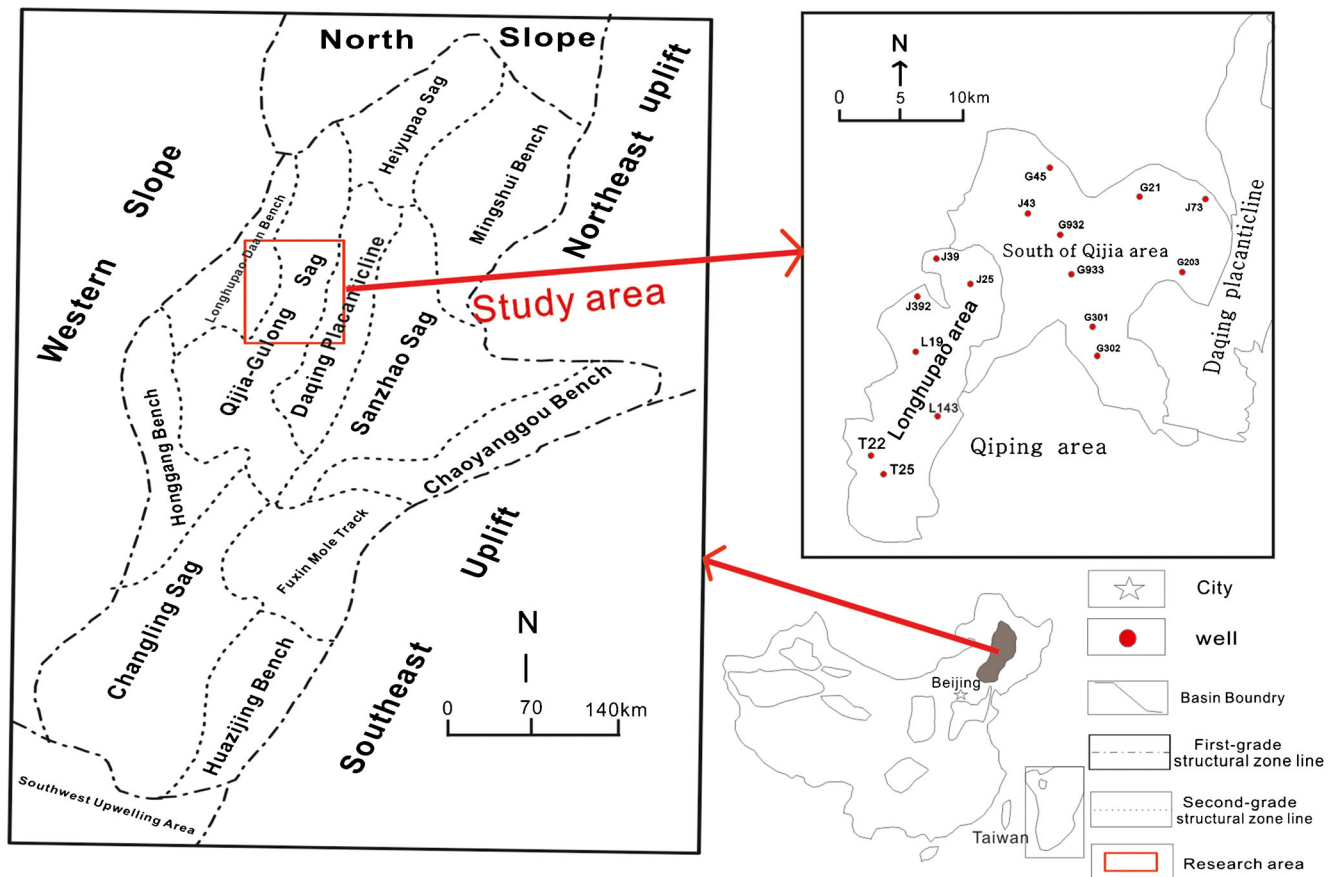


Fig. 1 Location of the study area (Yilin et al. 2016; Hang 2018)

statistical interval (a total of 28 samples) according to the rule that permeability changes from large to small, Thus, each sample selected is representative and all types of reservoirs in the study area are included.

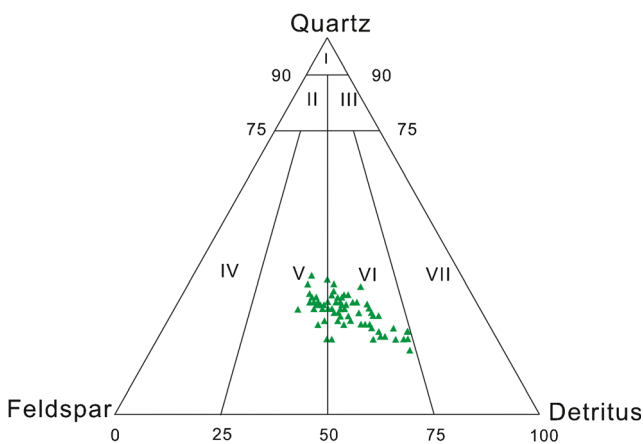


Fig. 2 Triangular chart of clastic composition in the study area (Ming 2016)

Methods of grading and evaluating pore throats

For tight reservoirs, the size and homogeneity of pore-throat distribution are significance for future exploration and development. Selecting a method of accurately determining the distribution and connectivity of pore throats requires careful consideration and can be contentious. Scanning electron microscopy (SEM) can directly characterise the pore throat, but its characterisation range is narrow and can only be used as a means of auxiliary evaluation. Micro-nano-computed tomography (CT) has some advantages in studying the connectivity of pore throats, but the test is expensive, and its resolution is limited. The most accessible and commonly used assessment method is high-pressure mercury injection. In this procedure, the oil filling process is simulated by injecting mercury into the sample. The curve formed by the relationship between mercury saturation and capillary pressure is analysed to characterise the pore-throat system comprehensively and accurately. Based on the classification of pores and throats, the mathematical expectation and variance are used to evaluate each class of pores and throats and to determine the size and distribution uniformity of the type of pore and throat. Based on the

pore-throat radius and mercury injection volume increment in the corrected mercury injection data, the mean parameters ($\overline{r_{j-k}}$) and homogeneous parameters (S^2) of pores and throats at different levels were calculated according to the expectation (Formula 1) and variance (Formula 2). The mean parameter, $\overline{r_{j-k}}$, is the expectation of a set of data, which can be used to measure the size of the pore-throat radius at all levels. The homogeneous parameter, S^2 , is the variance of a set of data, reflecting the degree of data fluctuation, which can be used to reflect the uniformity degree of pore-throat distribution, concentration or dispersion.

$$\overline{r_{j-k}} = \frac{\sum_{i=k}^j r_i \cdot \Delta V_{Hgi}}{\sum_{i=k}^j \Delta V_{Hgi}} \quad (1)$$

$$S^2 = \frac{\sum_{i=k}^j (r_i - \overline{r_{j-k}})^2}{j-k+1} \quad (2)$$

In these equations, r_i is the radius of the pore throat, and r_k and r_j are the critical radii of pore throats at all levels. ΔV_{Hgi} is the corresponding incremental volume of mercury injection; $\overline{r_{j-k}}$ is the mean parameter (the expected value of the pore-throat radius at all levels); and S^2 is the homogeneous parameter (variance of pore throat at all levels).

Results and discussion

Microscopic classification of pore throats

Common characterisation techniques of microscopic pore throats can be roughly divided into direct observation techniques (such as SEM, casting sheet and micro-nano CT) and indirect measurement techniques (such as high-pressure mercury injection, constant velocity mercury injection, low-temperature nitrogen adsorption and nuclear magnetic resonance) (Qiang et al. 2018). Although direct observation technology can directly characterise the shape and size of a microscopic pore throat, it is limited to only one point and it requires much statistical work to accurately evaluate a pore throat. This evaluation is not simple and is mainly used to corroborate other analysis results. Of the indirect measurement technologies, only high-pressure mercury injection has a wide range of characterisation (nanometer–micron), which can characterise the full pore size of a tight sandstone reservoir.

Looking at the curve generated from high-pressure mercury injection observations shows several different

insights, but the most significant is the inflection point. From the point of view of mathematical geometry, the inflection point represents a great change in slope; in terms of the process of mercury injection, the change of mercury intake represents a change in pore development degree. The injection curve represents pores, and the withdrawal curve represents the throat. By analysing the morphological characteristics of the mercury curves, especially the location of any inflection points, the author classified the 28 samples of tight sandstone in the Gao 3 section of the study area by pore system and throat system. The results show that there are inflection points on both the mercury injection curve and the mercury withdrawal curve, and there are two inflection points on the mercury injection curve. As the reservoir's physical properties change, the inflection point gradually rises; that is, samples with different porosity and permeability have different pore systems. Based on the location of the inflection points (Figs. 3 and 4), the pore systems have been divided into three types: macropore, transitional pore and micropore. The boundary of the pore-throat system of each level is determined by combining the corresponding capillary pressure and relative permeability. Xinghe (2009) pointed out that permeability is less than 10 mD in a low-permeability reservoir. Unconventional reservoirs are defined as having low porosity (< 10%) and low air permeability (< 1 mD) (Caineng 2015). On this basis, the pore-throat boundary is determined according to the actual geological conditions of the study area. When the permeability is greater than 10 mD, it is a conventional reservoir with good pore-throat connectivity. Figure 3a shows that the capillary pressure at the inflection points is successively 0.1 MPa and 1 MPa for this kind of reservoir. When permeability is between 1 and 10 mD, the reservoir is classified as a low-permeability reservoir. Figure 3b shows that the capillary pressure at inflection points is successively 0.1 MPa and 1 MPa for this kind of reservoir. Permeability less than 1 mD is defined as an unconventional reservoir. A large number of such reservoirs exist in the Gao 3 section of the study area. Six unconventional reservoirs with different physical properties were analysed using mercury injection (Fig. 4). For all reservoirs of this type, the ordinates of the two inflection points were stable at 2 MPa and 10 MPa, but when the permeability decreased to $0.04 \times 10^{-3} \mu\text{m}^2$, the first inflection point overlapped with the second inflection point, so that there was a single inflection point with a vertical coordinate of approximately 10 MPa. So, this kind of reservoir can be further divided into class I (1–0.04 mD) and class II (<mD). Capillary pressure at inflection points is successively 2 MPa and 10 MPa for class I and 10 MPa for class II.

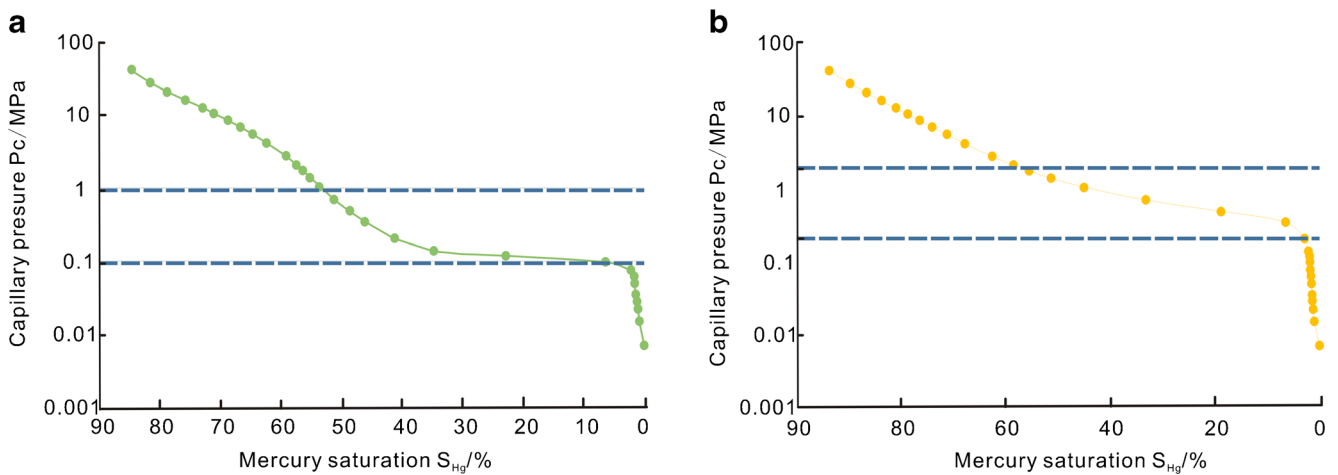


Fig. 3 Inflection point on the mercury injection curve of conventional and low-permeability reservoirs: **a** Jin38, 1785.6 m, Gao 3 section, 31.8 mD; **b** Du36, 1736.6 m, Gao 3 section, 5.26 mD

According to the Laplace–Washburn equation, the radius of the pore throat corresponding to the inflection point can be calculated as

$$P_c = \frac{2\sigma \cos\theta}{R} \tag{3}$$

where P_C is capillary pressure, dyn/cm²; θ is liquid contact angle of mercury; σ is surface tension of mercury, dyn/cm²; and R is pore-throat radius, cm.

If the P_C is measured in MPa, R is measured in μm and the liquid contact angle of mercury is 146° , then the surface tension of the mercury is $4.85 \times 10^{-1} \text{ N/m}$; $1 \text{ dyn/cm}^2 = 0.1 \text{ Pa}$. Therefore,

$$R = \frac{0.814}{P_c} \tag{4}$$

The principle of the mercury injection experiment is using mercury to simulate the filling process of oil and gas and then characterising the full pore size of the reservoir material.

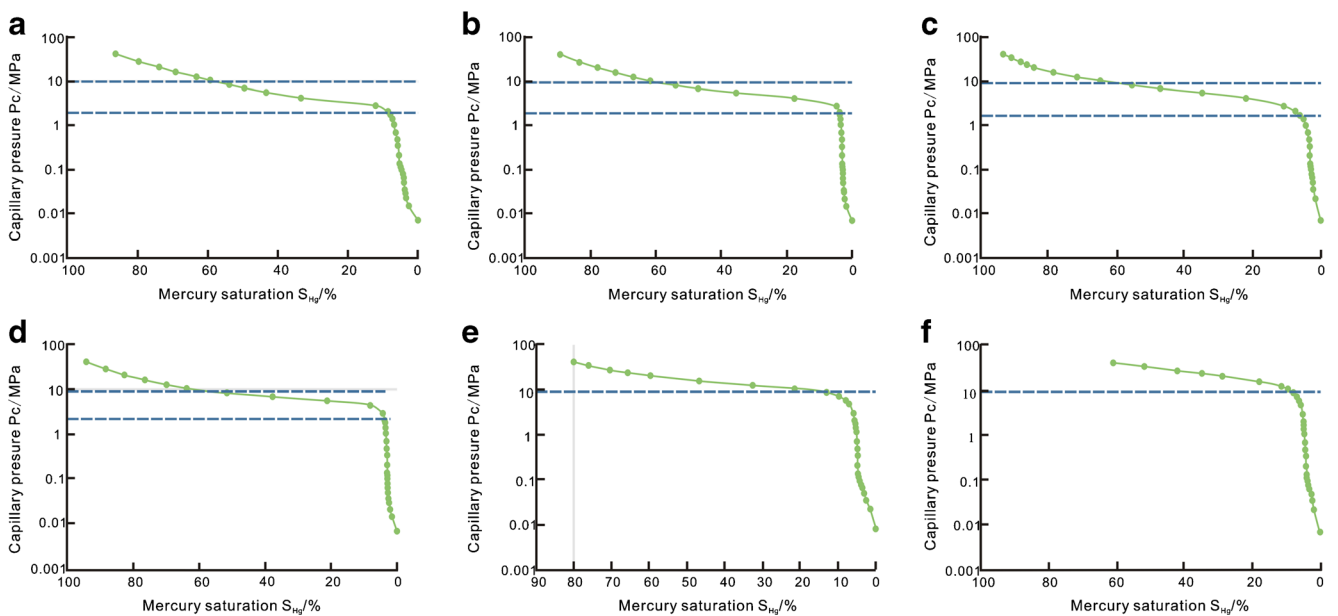


Fig. 4 Inflection point on the mercury curve of unconventional reservoirs: **a** Xin83, 1906.23 m, Gao 3 section, 0.44 mD; **b** Xin83, 1928.03 m, Gao 3 section, 0.1 mD; **c** Xin98, 1704 m, Gao 3 section, 0.07 mD; **d** Xin83, 1928.77 m, Gao 3 section, 0.05 mD; **e** Jin86, 1923.93 m, Gao 3 section, 0.04 mD; **f** Jin86, 1944.60 m, Gao 3 section, 0.03 mD

Table 1 The classification standards of all levels of reservoirs

Permeability Pore level	> 10 (Conventional reservoir)	1–10 (Low-permeability reservoir)	< 1 (Unconventional reservoirs)	
			Class I (> 0.04)	Class II (< 0.04)
Macropore (μm)	> 8.14	> 4.07	> 0.407	> 0.0814
Transitional pore (μm)	8.14–0.814	4.07–0.407	0.407–0.0814	/
Micropore (μm)	< 0.814	< 0.407	< 0.0814	< 0.0814

Experimental data were collected at the fluid mechanics laboratory of the Exploration and Development Research Institute of Daqing Oilfield Company Ltd. Oil, and gas industry standard SY/5346-1994 was used to determine the rock capillary pressure curve.

The corresponding pore-throat radius can be obtained by substituting the capillary pressure at the inflection point into the Formula 1 (Table 1).

According to the theory characterising the pore throat using a mercury withdrawal curve and statistics and analysis, it was found that there were two inflection points in common, and that the ordinate of the inflection point remained basically unchanged. The corresponding capillary pressures at the inflection points were 1 MPa and 10 MPa (Fig. 5). According to the Laplace–Washburn equation, the radius of the throats corresponding to 1 MPa and 10 MPa can be calculated as 0.814 μm and 0.0814 μm , respectively. Therefore, the throats of the study area can be divided into three types: large throats (> 0.814 μm), medium throats (0.0814–0.814 μm) and small throats (< 0.0814 μm).

Pore-throat grading

The author refers to the international mainstream classification of the pore throats. Based on the mercury injection curve combined with the actual geology of the Gaotaizi reservoir, pores in the study area are divided into three types: macropores, transition pores and micropores. The main parameters used were the means of parameters and homogeneous parameters. Thin sections and an SEM analysis were used as supplementary methods of evaluating the porosity.

Based on the measured mercury injection pressure and the amount of mercury injected, per the corrected mercury injection data, the corresponding pore-throat radius can be calculated by using Formula 4. Using Formulas 2 and 1, the mean parameter and homogeneous parameter of each pore throats in each sample can be obtained (Table 2). Based on the relative permeability of each block, a reservoir type is assigned and the characteristics of the pore throats of each reservoir are analysed. We know that although the throat is the main influencing factor of permeability, porosity cannot be completely ignored. Therefore, all effective pore-throat systems in the tight sandstone reservoir jointly determine the relative permeability. Based on the reasonable pore-throat classification, the correlation between the permeability and grading parameters (mean parameters and homogeneous parameters) was analysed for all levels of pore throat in the same reservoir to determine the relative influence of all levels of pore throat on permeability.

Evaluation of pore throats in a conventional reservoir

A histogram of pore-throat distribution in the sample was produced based on the mercury injection volume at all levels of pore throats in the mercury injection data of the reservoir (Fig. 6). Here, we see that the peak value of the pore-throat distribution in this type of reservoir is concentrated in the transition pores (0.814–8.14 μm). Additionally, with an increase in permeability, the content of macropores gradually increases, the transition pores first increase and then decrease, and the content of micropores continues to decrease. Observing the sample in the thin section (Fig. 7) and SEM (Fig. 8) analyses, the pore

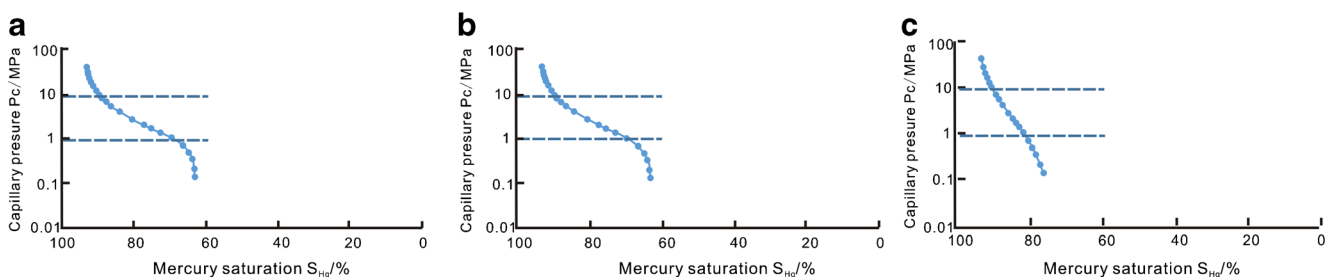


Fig. 5 Inflection point on the mercury withdrawal curve: **a** Jin50, 2025.6 m, 0.06 mD; **b** Xin98, 1962.2 m, 0.18 mD; **c** Du36, 1736 m, 5.26 mD

Table 2 Mean parameters and homogeneous parameters of all levels of pore throats at all levels of reservoirs

Well number	Depth (m)	Mean parameters (μm)		Homogeneous parameters (μm ²)		Permeability (mD)	Reservoir category
		Macropore	Transitional pore	Macropore	Transitional pore		
Jin 50	2133.00	10.570	3.947200	0.194	4.9239	45.7	Conventional reservoir
Gu 72	2018.41	9.611	2.8040	0.0499	5.02	170	
Gu 72	2016.83	9.629	3.30528	0.0495	3.30	216	
Du 37	1711.32	39.692	2.9567	0.1664	4.860	26.4	
...
Du 36	1733.47	32.068	1.29237	0.1432	0.661	5.26	Low-permeability reservoir
Jin 95	1861.78	36.625	1.8960	0.135	1.65	6.69	
Du 37	1688.77	646.172	1.65898	0.012	0.680	1.95	
...	
Jin 50	2025.60	23.691	0.13835	0.055	0.016	0.06	Unconventional reservoirs (class I)
Xing 98	1962.20	4.65	0.20197	0.053	0.011	0.18	
Xing 98	1704	18.564	0.1687	0.0534	0.013	0.07	
Xing 83	1926.50	30.773	0.1911	0.047	0.0116	0.44	
...
Jin 50	2096.60	2.070	...	0.051	...	0.04	Unconventional reservoirs (class II)
Ji 83	1954.21	30.793	...	0.040	...	0.02	
Xing 98	1689.4	0.744	...	0.040	...	0.01	
...	

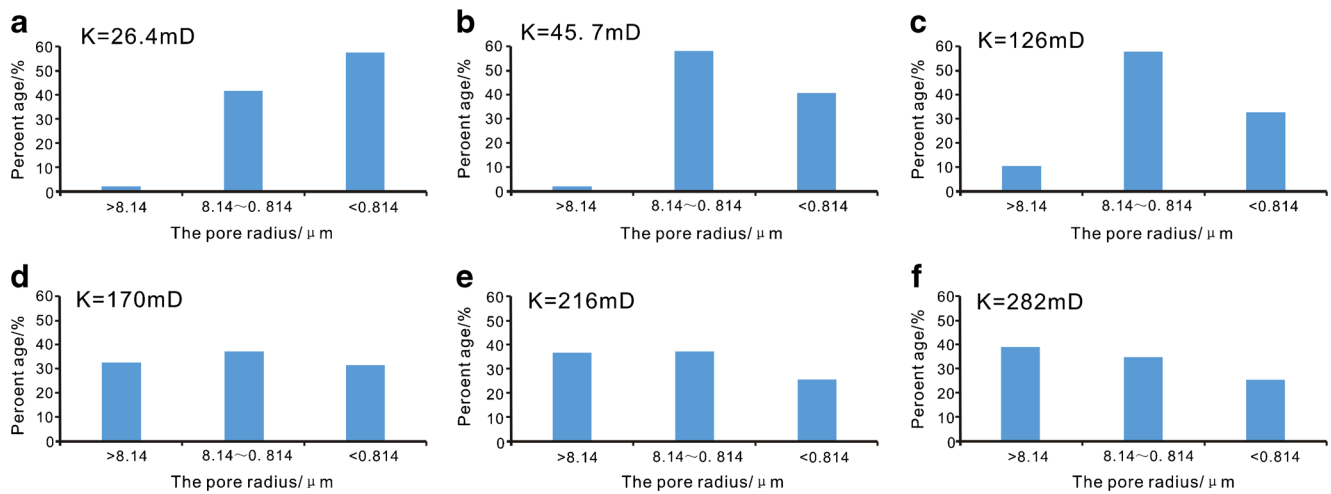


Fig. 6 Histograms of pore-throat distribution in a conventional reservoir: a Du37, 1711.32 m; b Jin 50, 2133.00 m; c Du38, 1690.45 m; d Gu72, 2018.41 m; e Gu72, 2016.83 m; f Du38 1690.76 m

throats at all levels can be clearly identified; the fidelity of these images allows us to confirm that pore throats in this type of reservoir are correctly classified.

To further define the relationship between pore throats and permeability, seven samples were selected from conventional reservoirs and grading parameters (the mean parameter and the homogeneous parameter) were analysed for all levels of pore throats (Table 3). A correlation analysis with permeability was made (Fig. 9) to determine the strength of the relationship between all categories of pore throats and permeability.

According to the correlation diagram between the grading parameters (mean and homogeneous) of all categories of pore throats and permeability (Fig. 9), the correlation between transition pores and permeability is not strong. The mean parameters are distributed between 3 and 5 μm , whereas the homogeneous parameters are concentrated around 5 μm^2 . According to Fig. 9a and c, the mean parameters of macropores show a negative correlation with permeability, and the mean parameters of micropores show a positive correlation with permeability. The results are consistent with the definition of the mean parameter, which reflects the average

size of the pore throat and that relatively large pores facilitate fluid seepage. The reason why the mean parameter of macropores is negatively correlated with permeability is that the effect of micropores on permeability is much stronger than that of macropores. According to Fig. 9d and f, the homogeneous parameters of macropores and micropores tend to decrease with the increase of permeability. Therefore, the homogeneous degree of macropores and the homogeneous degree of micropores have similar effects on permeability.

Evaluation of pore throats in a low-permeability reservoir

It can be seen from Fig. 10 that the pore distribution of this type of reservoir is mainly concentrated in transition pores (0.407–4.07 μm) and micropores (< 0.407 μm), and the macropores are almost negligible. With the increase of permeability, the number of transition pores gradually increased and the number of micropores gradually decreased. The resolution of the thin section can no longer characterise all levels of pore throats, but they can be clearly characterised when viewed by SEM (Fig. 11).

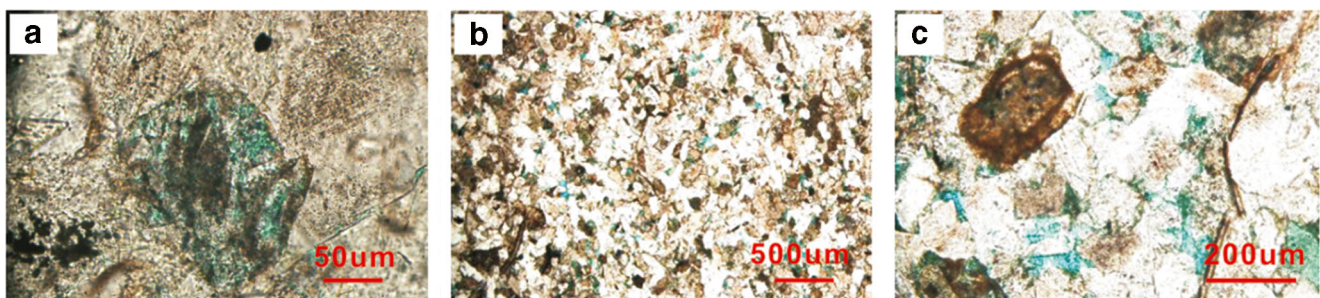


Fig. 7 Macropores and transitional pores in conventional reservoirs (thin section): a Jin 50, 2133.00 m; b Du 37, 1711.32 m; c Du 38, 1699.45 m

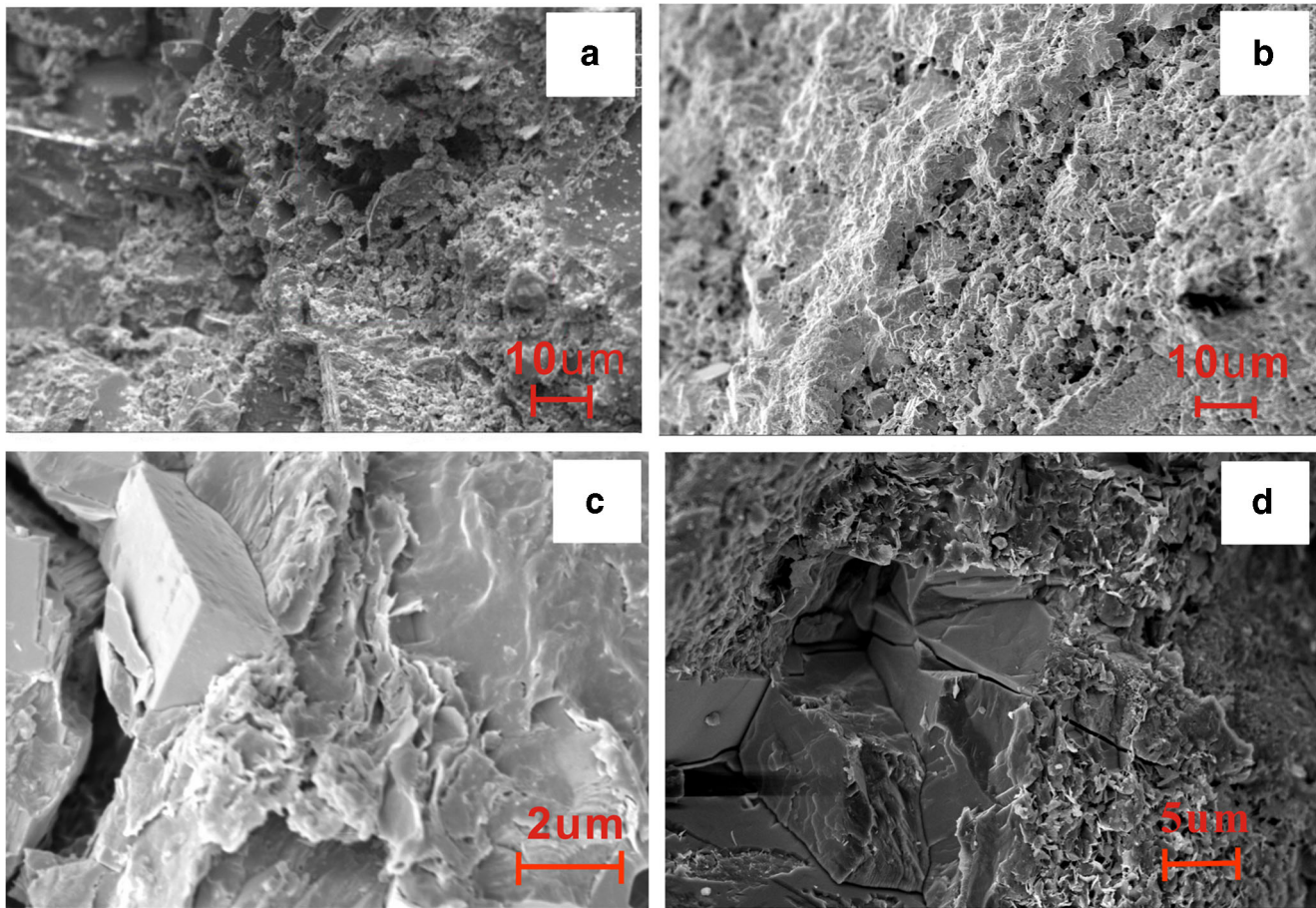


Fig. 8 Microscopic characteristics of pores and throats in conventional reservoirs (SEM): **a** Jin 50, 2133.00 m; **b** Du 38, 1699.45 m; **c** Du 37, 1711.32 m; **d** Gu 72, 2016.83 m

To further clarify the relationship between pore throat and permeability for low-permeability reservoirs, five samples were selected from low-permeability reservoirs, and the grading parameters (mean parameter and homogeneous parameter) of all levels of pore throats were calculated (Table 4). Then, the correlation permeability was calculated (Fig. 12)

to determine the strength of the relationship between all categories of pore throats and permeability.

According to Fig. 12(a, d), the correlation among the mean parameters and the homogeneous parameters of the macropores and the permeability is weak and not significant in the present study. In Fig. 12(b, e, c, f), the grading

Table 3 Grading parameters and permeability of conventional reservoirs

Well number	Depth (m)	Mean parameters (μm)			Homogeneous parameters (μm^2)			Permeability (mD)
		Macropore	Transitional pore	Micropore	Macropore	Transitional pore	Micropore	
Du 37	1711.32	39.692	2.9567	0.16640	568.973	4.8600	0.03400	26.4
Jin 38	1785.60	16.172	4.9716	0.15160	558.974	7.0673	0.03460	31.8
Jin 50	2133.00	10.57	3.9472	0.1942	716.503	4.9239	0.03302	45.7
Du 38	1699.45	16.44	4.9977	0.17597	16.443	4.9977	0.1759	126
Gu 72	2018.41	9.6113	4.2710	0.2207	590.06	5.02175	3.1482	170
Gu 72	2016.83	9.629	3.305	0.04956	9.62947	3.3052	0.04956	216
Du 38	1701.09	11.66	4.2457	0.21662	672.521	5.3164	0.0339	282

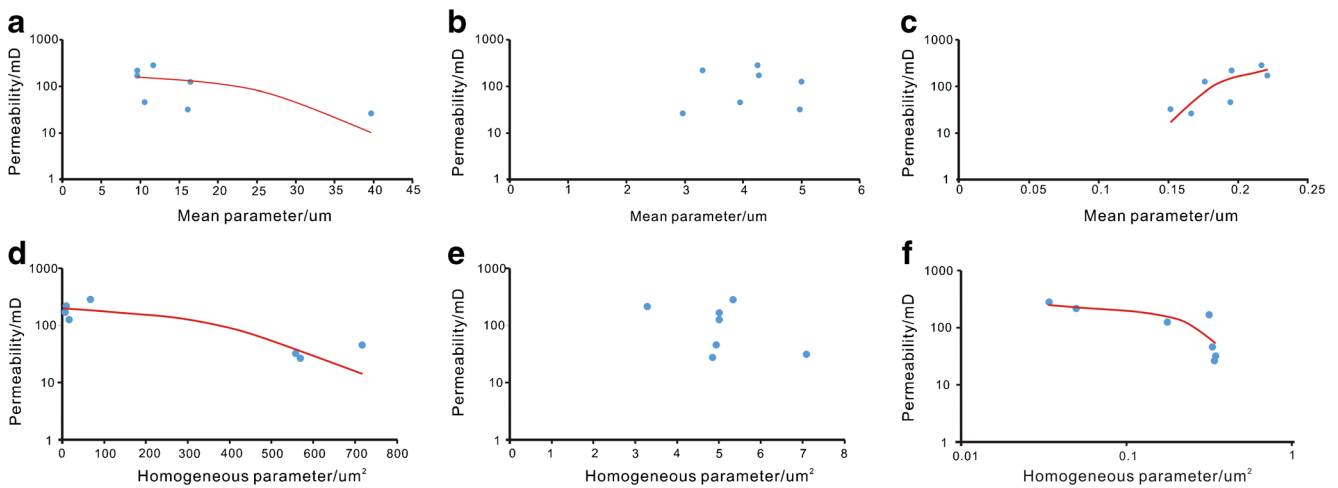


Fig. 9 Correlation between the grading parameters and permeability in conventional reservoirs: **a** correlation diagram between the mean parameter of macropores and permeability; **b** correlation diagram between the mean parameter of the transition pores and permeability; **c** correlation diagram between the mean parameter of micropores and

permeability; **d** correlation diagram between the homogeneous parameter of macropores and permeability; **e** correlation diagram between the homogeneous parameter of the transition pores and permeability; **f** correlation diagram between the homogeneous parameter of micropores and permeability

parameters of transition pores show a good positive correlation with permeability, whereas the grading parameters of micropores show a negative correlation with permeability. The main reason for the negative correlation between the mean parameter of transition pores and permeability is that the effect of the mean parameter of transition pores on permeability is much stronger than the effect from micropores. It can be seen from Fig. 12(e, f) that the homogeneous parameters of transition pores are positively correlated with permeability, whereas the homogeneous parameters of micropores are negatively correlated with permeability. According to the definition of the homogeneous parameter (to measure the concentration or dispersion degree of pore-throat distribution), the larger its value is, the more dispersed the pore-throat distribution is, and the harder it is for fluid to flow. The effect of micropore homogeneity on permeability is much stronger than that of transition porosity; this results in a positive correlation between homogeneous parameters and permeability.

Evaluation of pore throats in an unconventional reservoir

According to the relative size of gas permeability samples, many unconventional reservoirs have been developed in the

study area. This kind of reservoir should be the focus of future research. Based on the relative size of the permeability, the reservoir can be divided into class I (permeability is greater than 0.04 mD and there are a large number of developments in the study area) and class II (permeability is less than 0.04 mD and there is only one individual sample). Because a class II reservoir is too tight, the error of the test value is too large, because the study area contains so few of these reservoirs. As this article is based on the tightest reservoir samples to correct for artificial reservoir space, class II calculations can cause greater error; this article only studied class I reservoirs. According to Fig. 13, the pore throat of this type of reservoir is mainly distributed in the transition pores (0.0814–0.407 μm), but the content of micropores and macropores cannot be ignored, and it fluctuates as permeability changes. The micropore throats of such reservoirs can no longer be identified in thin section. The shape and size of the pore throat can only be accurately identified with the help of ultra-high resolution SEM (Fig. 14).

To further clarify the relationship between pore throats and permeability, 13 samples from unconventional reservoirs (class I) were selected, and grading parameters (mean and homogeneous parameters) were calculated for all

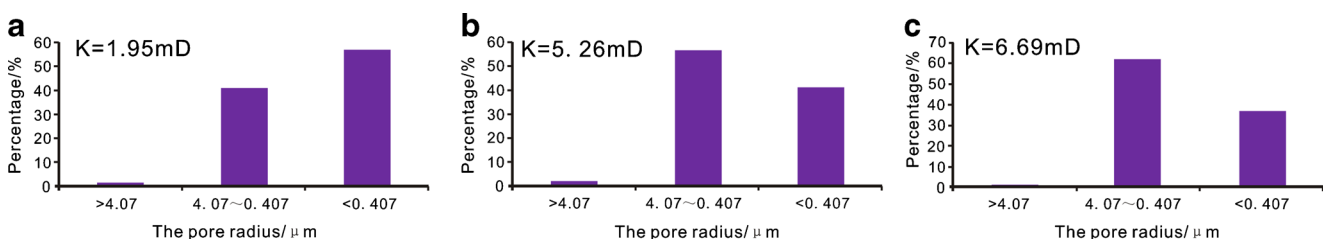


Fig. 10 Histograms of pore-throat distribution in low-permeability reservoirs

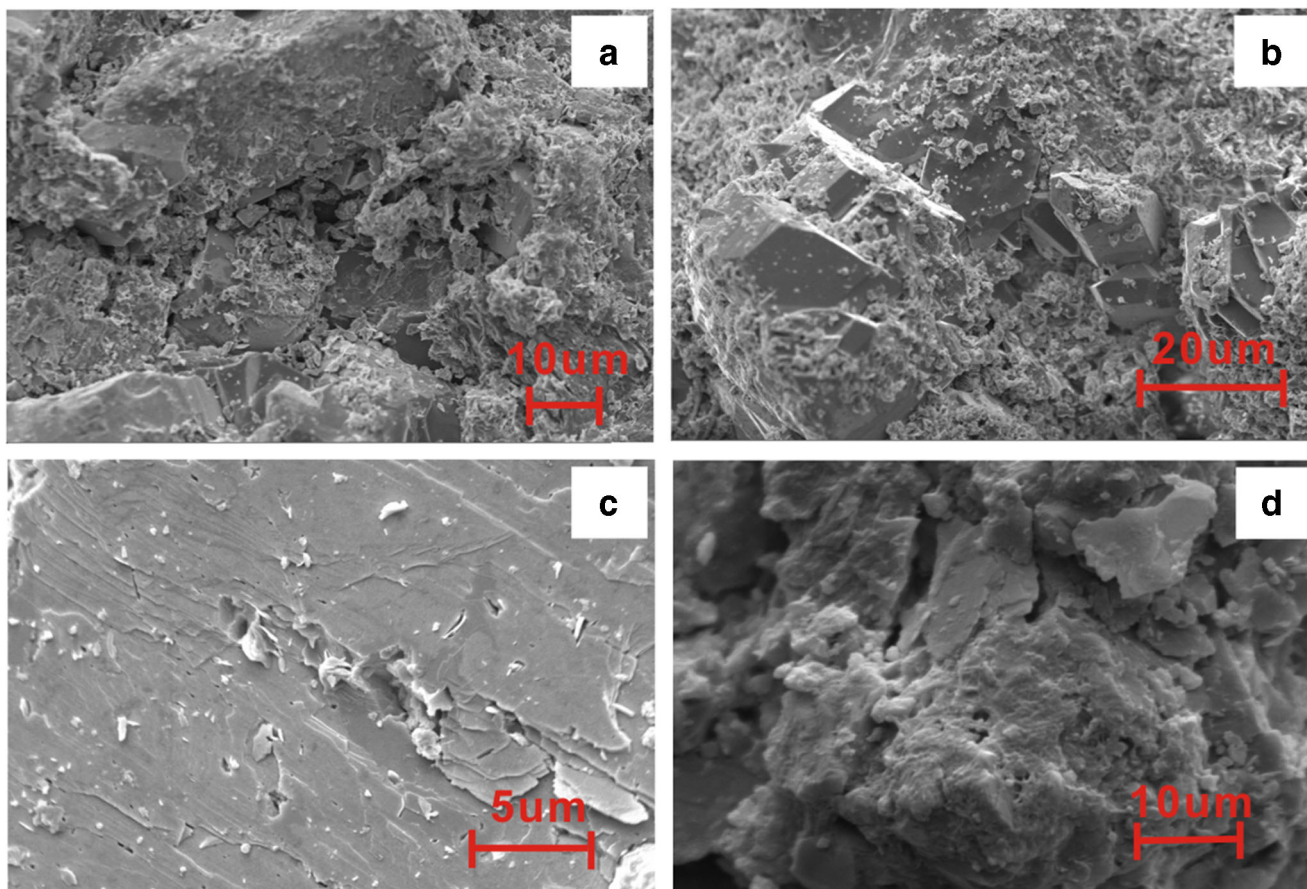


Fig. 11 The microscopic characteristics of all levels of pore throats in low-permeability reservoirs as viewed with SEM: **a** Du 36, 1733.47 m; **b** Jin 95, 1861.78 m; **c** Du 37, 1688.77 m; **d** Du 36, 1733.47 m

classifications of pore throats (Table 5). A correlation analysis with permeability was then conducted (Fig. 15) to determine the strength of the relationship between pore throats and permeability.

According to Fig. 15(a–c), the mean parameters of macropores and micropores show strong negative correlation with permeability, whereas the mean parameters of transition pores show a strong positive correlation with permeability. This indicates that the effect of the mean parameters of transition pores on permeability is much stronger than that of the

mean parameters of macropores and micropores; so, the mean parameters are negatively correlated with permeability. According to the Fig. 15(d–f), the homogeneous parameters of macropores, transition pores and micropores all show a negative correlation with permeability. This result is consistent with the definition of homogeneous parameters. Macropores, transition pores and micropores jointly affect the permeability. However, because the pore-throat distribution of this kind of reservoir is mainly concentrated in the transition pores, the transition pores may be more important.

Table 4 Grading parameters and permeability of all levels of pore throats in low-permeability reservoirs

Well number	Depth (m)	Mean parameters (µm)			Homogeneous parameters (µm ²)			Permeability (mD)
		Macropore	Transitional pore	Micropore	Macropore	Transitional pore	Micropore	
Du 36	1 738.47	1.5923	0.14323	0.16640	524.0103396	0.861825913	0.01289557	5.26
Jin 95	1 863.78	1.8960	0.13524	0.15160	646.1720694	1.658980412	0.012692169	6.69
Du 37	1 688.77	1.1800	0.15856	0.1942	767.495332	0.680207265	0.050015146	1.95
Jin 86	1 995.20	1.9389	0.13692	0.17597	393.1751068	1.703249657	0.012784334	7.82
Jin 87	1 834.18	1.5385	0.15665	0.2207	351.1245643	0.823412047	0.023951319	2.89

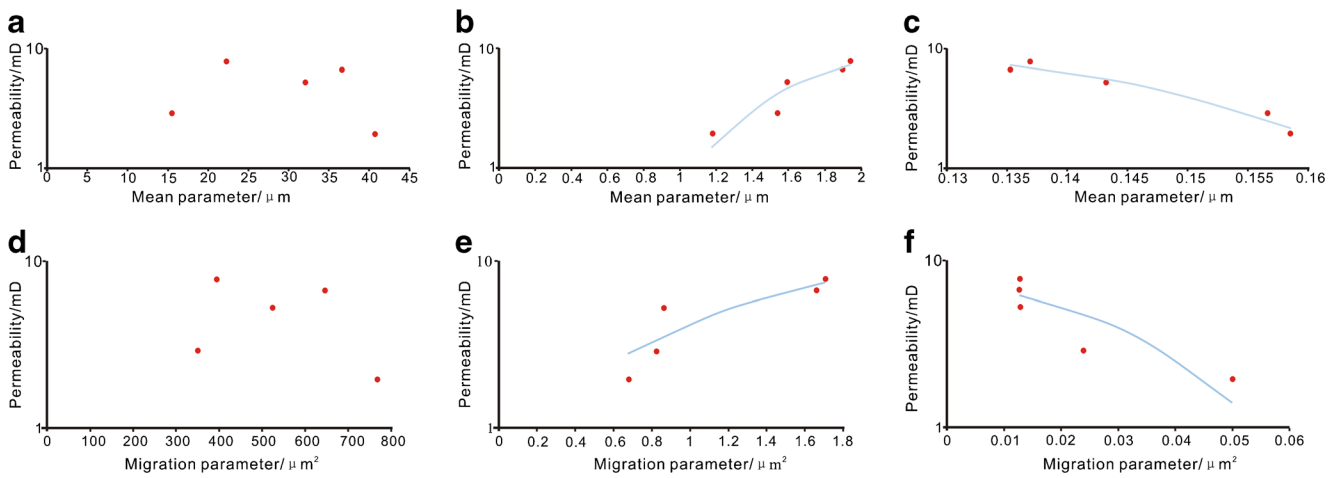


Fig. 12 Correlation diagram of pore-throat grading parameters and permeability in low-permeability reservoirs: **a** correlation diagram between mean parameters of macropores and permeability; **b** correlation diagram between the mean parameters of transition pores and permeability; **c** correlation diagram between mean parameters of micropores and

permeability; **d** correlation diagram between homogeneous parameters of macropores and permeability; **e** correlation diagram between homogeneous parameters of transition pores and permeability; **f** correlation diagram between homogeneous parameters of micropores and permeability

Comprehensive classification and evaluation of tight sandstone reservoirs

The mercury injection curves of all samples in the Gao 3 section of the study area were plotted on the same axes (Fig. 16), and the measured mercury injection curves were observed and summarised (Table 6). In Fig. 16a, the red curve at the bottom is the conventional reservoir, the purple curve at the middle is low-permeability reservoir, and the blue curve at the top is the unconventional reservoirs (class I). A large number of such reservoirs were developed in the study area.

Classification and evaluation of conventional reservoirs

The displacement pressure for this type of reservoir (Fig. 16d) ranged from 0.05 to 0.15 MPa, and the mercury

injection curve shows a long level section in the middle. However, when the mercury saturation reaches 50% of the reference value, it starts to rise sharply. Gas permeability is greater than 10 mD, and porosity is mostly between 15 and 25%. Based on the characteristics of the mercury curve (the inflection point) and the pore-throat classification scheme developed by domestic and foreign experts, the pore throats for this kind of reservoir are found to be divided into macropores (> 8.14 μm), transition pores (0.814–8.14 μm) and micropores (< 0.814 μm). The correlation between the grading parameters of various pores and permeability shows that the mean parameter of macropores has the greatest influence on permeability, followed by the homogeneous parameters of macropores and the homogeneous parameters of micropores.

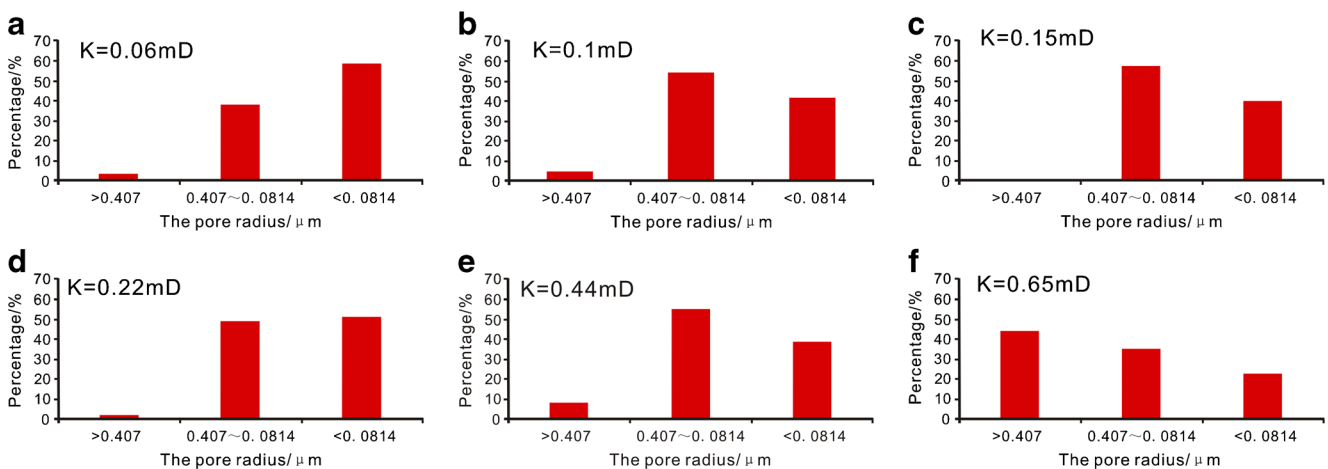


Fig. 13 Histograms of pore-throat distributions in unconventional reservoirs a Jin 50,2025

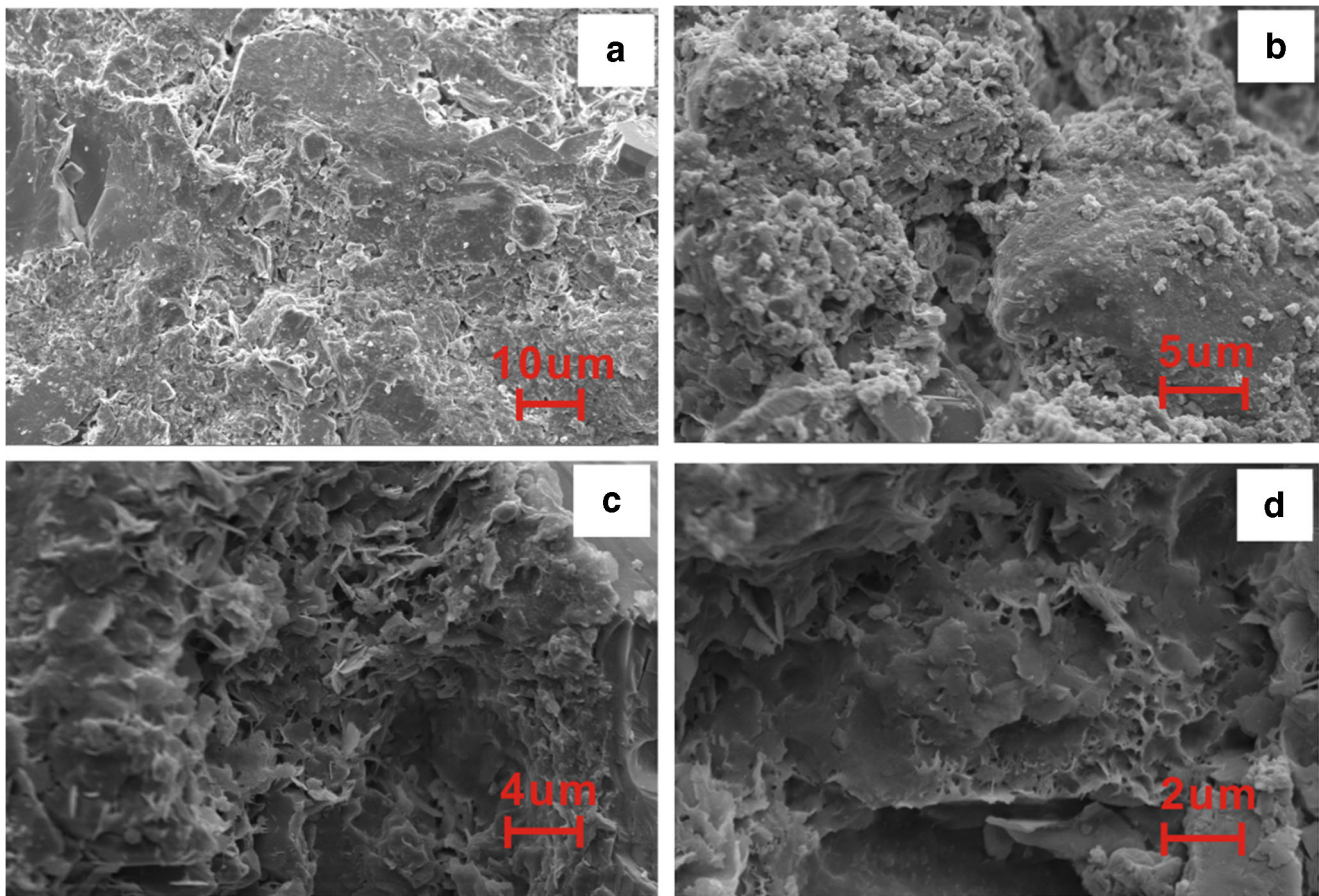


Fig. 14 Microscopic characteristics of various pores and throats in unconventional reservoirs (SEM): **a** Jin 50, 2025.60 m; **b** Xin 98, 1962.20 m; **c** Xin 98, 1704.00 m; **d** Xin 83, 1926.50 m

Classification and evaluation of low-permeability reservoirs

The displacement pressure of this kind of reservoir (Fig. 16c) ranges from 0.2 to 0.5 MPa; the inclination degree of mercury penetration curve is roughly the same; and

the middle section of the curve is not particularly obvious. Gas permeability is between 1 and 10 mD, and porosity is mostly between 13 and 23%. Based on the characteristics of the mercury curve (the inflection point) and the classification scheme of the pore throats

Table 5 Grading parameters and permeability of all categories of pore throats in unconventional reservoirs

Well number	Depth (m)	Mean parameters (μm)			Homogeneous parameters (μm ²)			Permeability (mD)
		Macropore	Transitional pore	Micropore	Macropore	Transitional pore	Micropore	
Jin 50	2025.60	23.691	0.1383	0.05517	448.233	0.016278	0.00042	0.06
Xing 98	1704.00	18.566	0.1687	0.0534	339.101	0.01322	0.00050	0.07
Xin 83	1928.03	44.299	0.1595	0.05031	1246.59	0.01423	0.00038	0.1
Jin 38	1871.80	23.514	0.1752	0.05058	437.475	0.0128	0.00037	0.15
Xing 83	2047.74	13.967	0.1486	0.05051	349.236	0.01538	0.00067	0.17
Xing 98	1962.20	4.655	0.2019	0.05347	323.6123	0.01107	0.00049	0.18
Jin 38	1828.40	10.034	0.2154	0.04437	377.336	0.01087	0.00038	0.22
Jin 87	1955.66	2.0499	0.2243	0.04816	365.428	0.01119	0.00041	0.38
Xing 83	1926.50	30.773	0.1911	0.04716	620.077	0.01167	0.00038	0.44
Gu 72	2029.24	1.06182	0.24413	0.0428486	371.179	0.01189	0.00037	0.58
...

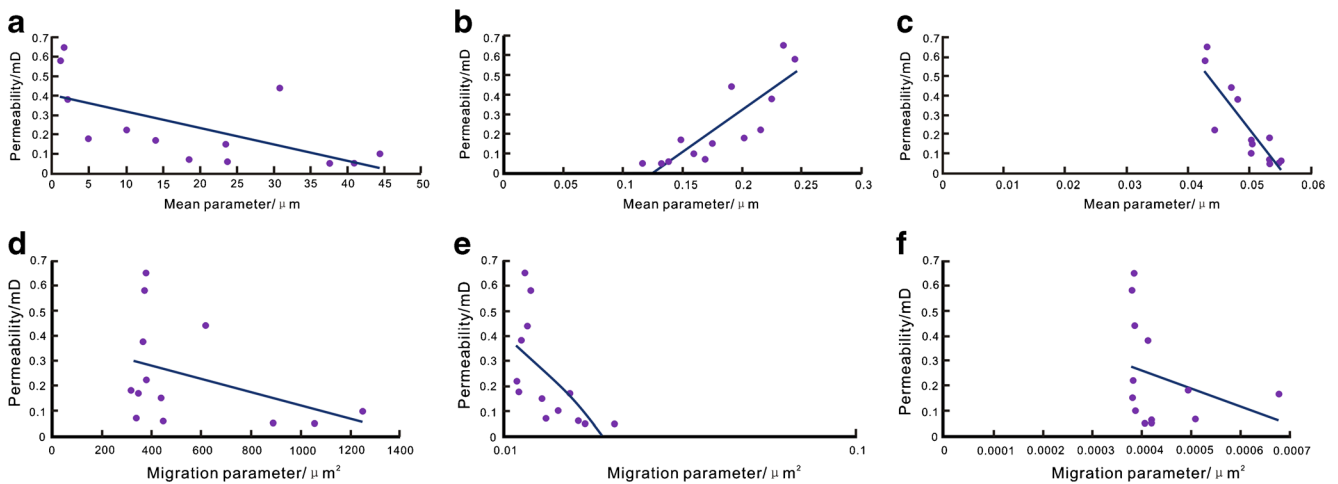


Fig. 15 Correlation diagrams for pore-throat grading parameters and permeability in unconventional reservoirs: **a** correlation diagram between mean parameters of macropores and permeability; **b** correlation diagram between mean parameters of transition pores and permeability; **c** correlation diagram between mean parameters of micropores and permeability; **d**

correlation diagram between homogeneous parameters of macropores and permeability; **e** correlation diagram between homogeneous parameters of transition pores and permeability; **f** correlation diagram between homogeneous parameters of micropores and permeability

of domestic and foreign experts, the pore throats of these reservoirs were divided into macropores ($> 4.07 \mu\text{m}$), transition pores ($0.407\text{--}4.17 \mu\text{m}$) and micropores ($< 0.814 \mu\text{m}$). The peak values of pore distribution are mainly concentrated in the transition pores and micropores. The correlation between all levels of pore throats and permeability indicates that the mean parameter of transition pores had the strongest influence on permeability, and the influence of homogeneous parameters of micropores on permeability is stronger than the other pore-throat parameters.

Classification and evaluation of unconventional reservoirs (class I)

The displacement pressure for this type of reservoir (Fig. 16b) ranges from 0.7 to 7 MPa, and the maximum mercury saturation gradually decreases with the increase of displacement pressure. The gas permeability is between 0.04 and 1 mD, and the porosity is between 7.8 and 16.8%. Based on the characteristics of the mercury injection curve (the inflection point) and the pore-throat classification scheme, the pore throats for this type of reservoir are divided into macropores ($> 0.407 \mu\text{m}$), transition pores ($0.0814\text{--}0.407 \mu\text{m}$) and micropores ($< 0.0814 \mu\text{m}$). The peak distribution of pore throats is mainly concentrated in the transition pores, but the numbers of micropores and macropores are still significant. A large number of such reservoirs were developed in the study area. The correlation between all levels of pore throats and permeability indicated that the mean parameter of transition pores had the strongest influence on permeability, and the relative size of permeability is

determined by the homogeneous parameters of macropores, transition pores and micropores (Table 6).

Conclusions

Based on the relative size of the permeability in the Gao 3 section of the study area, the reservoir can be divided into four categories: conventional reservoir ($K > 10 \text{ mD}$), low-permeability reservoir ($1 \text{ mD} < K < 10 \text{ mD}$), unconventional reservoir class I ($0.04 \text{ mD} < K < 1 \text{ mD}$) and unconventional reservoir class II ($K < 0.04 \text{ mD}$). Considering the characteristics of mercury injection curves of all kinds of reservoirs, the microscopic pore-throat characteristics were sorted into several categories. According to mercury injection curve inflection points and the classification schemes of domestic and foreign experts, the micropore throats are divided into three types: macropores, transition pores and micropores. Critical points were determined based on the ordinate at the inflection point and the capillary pressure combined with the Laplace–Washburn equation. The critical points of pore-throat classification in conventional reservoirs are $0.814 \mu\text{m}$ and $8.14 \mu\text{m}$. In low-permeability reservoirs, they are $0.407 \mu\text{m}$ and $4.07 \mu\text{m}$, and $0.0814 \mu\text{m}$ and $0.407 \mu\text{m}$ in unconventional reservoirs (class I). The accuracy of this classification was verified using thin sections and SEM. Unconventional reservoirs (class II) are too tight to promote significant permeability, and few of them have developed in the study area; so, this paper does not study them.

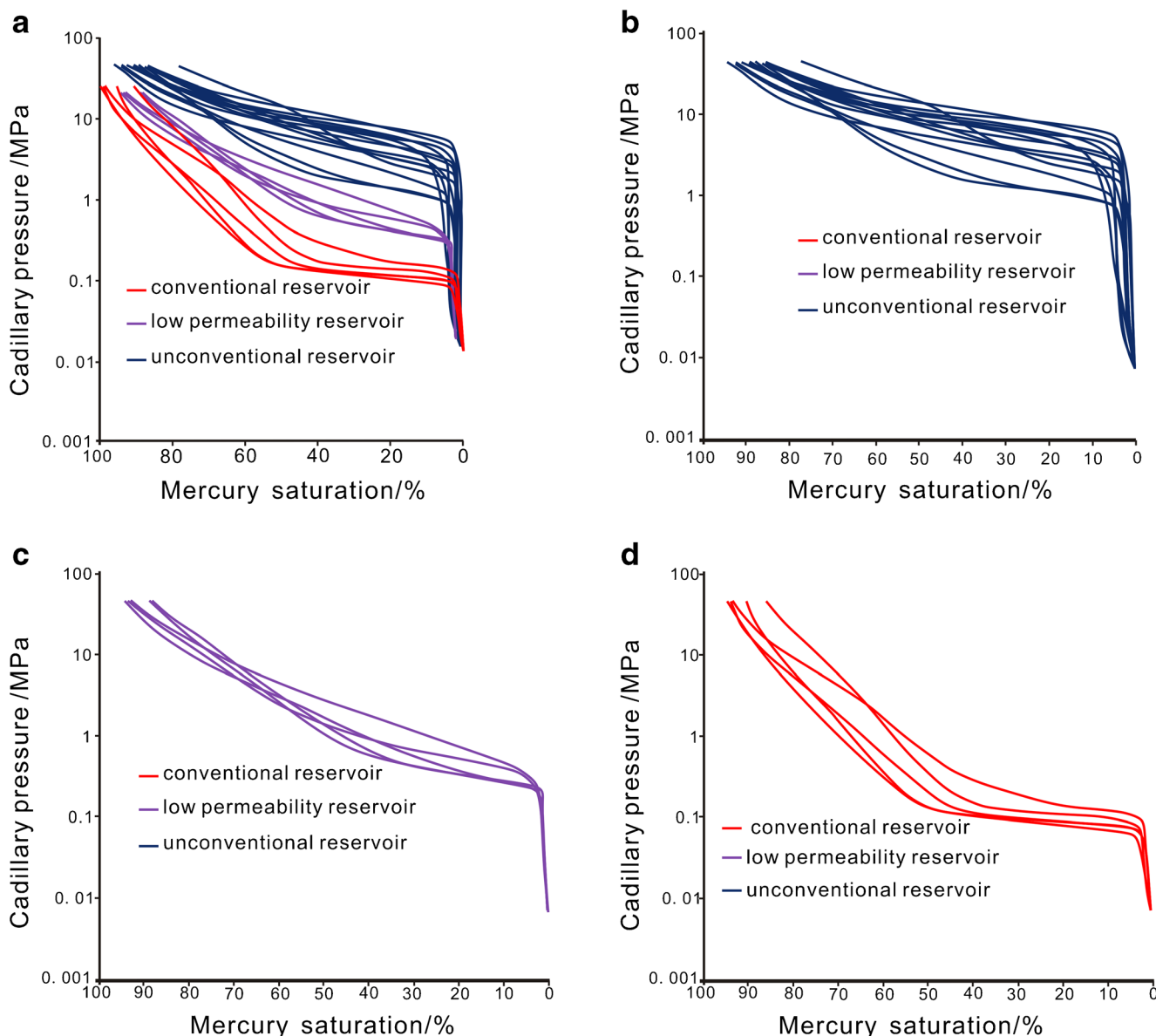


Fig. 16 Comprehensive classification of reservoirs in the study area: **a** mercury injection curves of various reservoirs; **b** mercury injection curves of unconventional reservoirs; **c** mercury injection curves in low-permeability reservoirs; **d** mercury injection curves in conventional reservoirs

The process of making the experimental sample is idealised, based on the mercury injection data of ultra-tight sandstone to eliminate the artificial storage space, and makes mercury injection data more reliable. Following the concepts of expectation and variance in mathematics, the grading parameters (mean parameters and homogeneous parameters) were introduced to characterise the sizes of pore throats and the concentration of pore-throat distribution. A correlation analysis was performed to determine the relationship between the grading parameters of pore throats and permeability. The results show that the main controlling factors of the permeability of conventional reservoirs include the mean parameter of macropores, the homogeneous parameter of macropores and the homogeneous parameter of micropores. The main

controlling factors of permeability for low-permeability reservoirs include the mean parameter of transition pores and the homogeneous parameter of micropores. The main controlling factors of permeability for unconventional reservoirs (class I) include mean parameters of transition pores, homogeneous parameters of macropores, homogeneous parameters of transition pores and homogeneous parameters of micropores.

Funding information This work was financially supported by the National Natural Science Foundation of China (Grant nos. 41572132 and 41772144), the Natural Science Foundation of Heilongjiang Province (Grant no. ZD2016007), and the Science Foundation for Young Scientists of Northeast Petroleum University (Grant no. 2018QNL-46).

Table 6 Comprehensive classification of reservoirs in the study area

Parameter	Reservoir category		
	Conventional reservoirs	Low-permeability reservoirs	Unconventional reservoirs (class I)
Displacement pressure (MPa)	0.05–0.15	0.2–0.5	0.7–7
Maximum incoming mercury saturation (%)	85–94	88–94	77–94
Permeability (mD)	> 10	1–10	0.04–1
Porosity (%)	15–25	13–23	7.8–16.8
Classification of pores (μm)	Macropores (> 8.14) Transition pores (0.814–8.14) Micropores (< 0.814)	Macropores (> 4.17) Transition pores (0.407–4.17) Micropores (< 0.814)	Macropores (> 0.407) Transition pores (0.0814–0.407) Micropores (< 0.0814)
Pore distribution peak	Transition pores	Transition pores and micropores	Transition pores
The main control factor of permeability	The mean parameter of macropores, the homogeneous parameters of macropores and homogeneous parameters of micropores	The mean parameter of transition pores and homogeneous parameters of micropores	The mean parameter of transition pores, homogeneous parameters of transition pores and homogeneous parameters of micropores

References

- Caineng Z, Shizheng T, Bing B, Zhi Y, Rukai Z, Lianhua H, Xuanjun Y, Guosheng Z, Songtao W, Zhenglian B, Lan W (2015) Differences and relations between unconventional and conventional oil and gas. *China Pet Explor* 20:1–16
- Chengzao J, Caineng Z, Jianzhong L, Denghua L, Ming Z (2012) Assessment criteria, main types, basic features and resource prospects of the tight oil in China. *Acta Pet Sin* 33:343–350
- Dullien FAL, Dhawan GK (1974) Characterization of pore structure by a combination of quantitative photomicrography and mercury porosimetry. *J Colloid Interface Sci* 47:337–349
- Hang F (2018) The tight reservoir microscopic classification of southern part of Qijia area in Songliao Basin. *IOP Conference Series: Earth Environ Sci* 113:012–025
- Hosseini M, Tavakoli V, Nazemi M (2018) The effect of heterogeneity on NMR derived capillary pressure curves, case study of Dariyan tight carbonate reservoir in the central Persian Gulf. *J Pet Sci Eng* 171: 1113–1122
- IUPAC (International Union of Pure and Applied Chemistry) (1972) Manual of symbols and terminology. *Pure Appl Chem* 31:578
- Jian X, Xiangjun L, Lixi L (2015) Experimental study on the pore structure characteristics of the Upper Ordovician Wufeng Formation shale in the southwest portion of the Sichuan Basin, China. *J Nat Gas Sci Eng* 22:530–539
- Jianzhong L, Bincheng G, Min Z, Tao Y (2012) Main types, geological features and resource potential of tight sandstone gas in China. *Nat Gas Geosci* 23:607–615
- Junjian Li, Cheng Baoyang, Liu Renjing, Meng Fanle, Liu Yang, Gao Yajun, Ma Kang, Jiang Hanqiao (2018) Microscopic mechanism of water sensitivity of pore-scale sandy conglomerate based on digital core. *Acta Petrolei Sinica*, 40(05):594–603.
- Liu A, Wang K, Zang J (2018) Relative permeability of gas for unconventional reservoirs. *Transp Porous Media* 124:289–307
- Ming Y (2016) The study of Gaotaizi oil layer's microscopic reservoir characteristics in Qijia area, Northeast Petroleum University 15
- Pengfei Z, Shangfang L, Junqian L, Haitao X, Wenhao L, Ping Z (2017) Characterization of shale pore system: a case study of Paleogene Xin'gouzui Formation in the Jiangnan basin, China. *Mar Pet Geol* 79:321–334
- Qiang Y, Yunfeng Z, Hang F, Meiling Z, Jun W, Shuling S, Han F, Rui H, Minghan G (2018) High pressure mercury injection and scanning electron microscopy applied to characterize micro-and nano-scale pore throats in tight sandstone reservoirs—a case study of the fourth member of Shahejie Formation in Y1176 block, Zhanhua Sag, Bohai Bay Basin. *Pet Geol Exp* 40:280–287
- Rui ZH, Lu J, Zhang ZE, Guo R, Ling KG, Zhang RL, Patil S (2017) A quantitative oil and gas reservoir evaluation system for development. *J Nat Gas Sci Eng* 42:31–39
- Shejiao W, Yuanjiang Y, Qiulin G, Saoyong W, Xiaozhi W (2014) New advance in resources evaluation of tight oil. *Acta Pet Sin* 35:1095–1105
- Shuangfang L, Junqian L, Pengfei Z, Haitao X, Guoli W, Jun Z, Huiming L, Zheng L (2018) Classification of microscopic pore throats and the grading evaluation on shale oil reservoirs. *Pet Explor Dev* 45:436–444
- Wang GW, Hao F, Chang XC, Lan CJ, Li PP, Zou HY (2017) Quantitative analyses of porosity evolution in tight grainstones: a case study of the Triassic Feixianguan formation in the Jiannan gas field, Sichuan Basin, China. *Mar Pet Geol* 86:259–267
- Weyl PK, Beard DC (1973) Influence of texture on porosity and permeability of unconsolidated sand. *AAPG Bull* 57:349–369
- XOJOT B B. Outburst of coal and coalbed gas//Shizhao S, Youan W(1996)translate. Beijing: China Industry Press.

- Xinghe Y (2009) Petroleum reservoir geology. Publishing House of Oil Industry, Beijing
- Yan S, Zhuo L, Zhengxue J, Qun L, Dongdong L, Zhiye G (2017) Progress and development trend of unconventional oil and gas geological research. *Pet Explor Dev* 44:638–648
- Yilin L, Yunfeng Z, Shuli Y, Lin C, Ming Y, Xiaoxiong T (2016) Characterization of the pore space in tight sandstone reservoirs from macroscopic and microscopic perspectives: a case study of Gaotaizi reservoir in Qijia area, the Songliao Basin. *Oil Gas Geol* 37:915–922
- Yunlong Z, Zhidong B, Zhao Y, Jiang L, Gong F (2017) Diagenesis and its controls on reservoir properties and hydrocarbon potential in tight sandstone: a case study from the Upper Triassic Chang 7 oil group of Yanchang Formation, Ordos Basin, China. *Arab J Geosci* 10:234
- Zhenhua R, Kehang C, Xiaoqing W, Ju W, Gang C, Ling KL, Shirish P (2018) A quantitative framework for evaluating unconventional well development. *J Pet Sci Eng* 166:900–905
- Zhu P, Zhu Z, Zhang Y, Sun L, Dong Y, Li Z, Chen M (2019) Quantitative evaluation of low-permeability gas reservoirs based on an improved fuzzy-gray method. *Arab J Geosci* 12:80